A two-scale method to include essential screw connection behaviour in two-way coupled fire-structure simulations

Qingfeng Xu and Hèrm Hofmeyer
Department of the Built Environment, Eindhoven University of Technology, Eindhoven, The Netherlands, and
Johan Maljaars
Department of the Built Environment, Eindhoven University of Technology, Eindhoven, The Netherlands and TNO, Delft, The Netherlands

Received 15 January 2023
Revised 27 May 2023
25 July 2023
Accepted 1 August 2023

Abstract

Purpose – Simulations exist for the prediction of the behaviour of building structural systems under fire, including two-way coupled fire-structure interaction. However, these simulations do not include detailed models of the connections, whereas these connections may impact the overall behaviour of the structure. Therefore, this paper proposes a two-scale method to include screw connections.

Design/methodology/approach – The two-scale method consists of (a) a global-scale model that models the overall structural system and (b) a small-scale model to describe a screw connection. Components in the global-scale model are connected by a spring element instead of a modelled screw, and the stiffness of this spring element is predicted by the small-scale model, updated at each load step. For computational efficiency, the small-scale model uses a proprietary technique to model the behaviour of the threads, verified by simulations that model the complete thread geometry, and validated by existing pull-out experiments. For four screw failure modes, load-deformation behaviour and failure predictions of the two-scale method are verified by a detailed system model. Additionally, the two-scale method is validated for a combined load case by existing experiments, and demonstrated for different temperatures. Finally, the two-scale method is illustrated as part of a two-way coupled fire-structure simulation.

Findings – It was shown that proprietary "threaded connection interaction" can predict thread relevant failure modes, i.e. thread failure, shank tension failure, and pull-out. For bearing, shear, tension, and pull-out failure, load-deformation behaviour and failure predictions of the two-scale method correspond with the detailed system model and Eurocode predictions. Related to combined load cases, for a variety of experiments a good correlation has been found between experimental and simulation results, however, pull-out simulations were shown to be inconsistent.

Research limitations/implications – More research is needed before the two-scale method can be used under all conditions. This relates to the failure criteria for pull-out, combined load cases, and temperature loads.

Originality/value – The two-scale method bridges the existing very detailed small-scale screw models with present global-scale structural models, that in the best case only use springs. It shows to be insightful, for it contains a functional separation of scales, revealing their relationships, and it is computationally efficient as it

The first author was partly financed by the China Scholarship Council, No. 2018-0861-0211, which is highly appreciated.

Journal of Structural Fire Engineering
Emerald Publishing Limited
2040-2317
DOI 10.1108/JSFE-01-2023-0005

allows for distributed computing. Furthermore, local small-scale non-convergence (e.g. a screw failing) can be handled without convergence problems in the global-scale structural model.

Keywords Two-scale method, Coupled fire-structure simulations, Screw connection, Structural failure, Spring element

Paper type Research paper

1. Introduction

Screw connections often serve as primary connectors in timber and steel structural systems, in the latter case especially so for thin-walled structures, e.g. cold-formed steel frames, and roofing and cladding systems (Kyvelou *et al.*, 2017, LaBoube and Sokol, 2002). This is because screws have appropriate strength, stiffness, and ductility to effectively and rapidly connect structural components via compression, tension, shear or combined actions: The screw connections are stressed due to loads on the structural system, e.g. wind, or by the increasing temperatures of a fire. The resulting behaviour, including elastic behaviour, elastoplastic behaviour and failure, depends on the connection's material properties, type, application pattern, etc. (EN ISO 898-1-2013 (2013). As such, many research projects have investigated the relationship between loads on the structural system and the behaviour of the screw connections (e.g. Lu *et al.*, 2011; Sivapathasundaram and Mahendran, 2016a). As another example of relevant research, Sivapathasundaram and Mahendran (2016b) conducted a series of pull-through tests, using roof battens connected by screws. Both (small-scale) screw connections and (global-scale) roof systems were tested, and suitable design rules were developed. Based on the Eurocode and existing research, Stamatopoulos and Malo (2020) reviewed the design guidelines for laterally-loaded threaded rods in wood, and provided theoretical expressions for their stiffness and capacity. Yan and Young (2012a, b) investigated screw connections under shear at elevated temperatures, and showed that the failure mode changed from bearing to shear when temperatures increased. A similar conclusion was found for sandwich panel systems by Cábová *et al.* (2021). Also, such shear connections can create large axial and flexural internal forces during a fire, leading to failure of the connections and subsequent progressive collapse of a (building) structure, as explained in Fischer *et al.* (2021).

Besides experiments and theories, also finite element analyses can be used to obtain knowledge on screw connection behaviour. For instance Huynh *et al.* (2020) investigated the load-deflection response of screw connections subjected to shear. By using solid finite elements for the screw, including the thread, their model successfully simulated various stress states, including fracture and failure. In another study, experimental screw connection tests were carried out and a non-linear explicit dynamic finite element model was developed. Both indicated the different failure modes for different load conditions, Roy *et al.* (2019). Regarding the load capacity of screw connections under fire, Lu *et al.* (2012) developed a 3D finite element model to predict the possible failure mechanisms of a screw connection for both ambient and elevated temperatures. It was also shown that the load-bearing capacity was highly temperature-dependent. The aforementioned studies indicate that a finite element model can replicate the different failure modes of a screw connection, for different load types. However, the research so far has focused on the small scale, mainly considering the screw and the directly adjacent components (e.g. plates). The role of a screw connection in the overall structural system is not so much modelled and studied.

Simulations exist for the prediction of the behaviour of building structural systems under fire. For instance, the object-oriented framework OpenSees has been further developed for fire conditions, and benchmarks and experiments have been successfully simulated (see Usmani *et al.*, 2012; Jiang *et al.*, 2015). Also research has been carried out specifically on two-way coupled fire-structure interaction (e.g. Feenstra *et al.*, 2018; De Boer *et al.*, 2019). However, these simulations do not include detailed models of the (screw) connections, despite their importance as mentioned above. This is because of the screw's small size and yet complex geometry, which requires a very

fine mesh related to the other structural components. Furthermore, each screw has a specific state of prescribed displacements, loads, temperatures, and strain history at each point in time, and consequently, computational costs are high. Some studies simplified the connections using the so-called component method, using a set of spring-like components (e.g. Zoetemeijer, 1974), with spring characteristics based on analytical or empirical models as shown by e.g. Swanson and Leon (2001) and Al-Jabri (2004). However, this component method cannot describe all essential types of behaviour, and their combinations, as presented in the next sections.

Therefore, this paper presents a two-scale method, which seeks to include all essential types of screw connection behaviour in coupled fire-structure simulations. As such bridging the gap between the existing very detailed small-scale screw models and the global-scale structural models, which in the best case only use springs. As will be shown, the method is insightful, for it contains a functional separation of scales, revealing their relationships. Also, it is computationally efficient as it allows for distributed computing. This is important because developments in high-performance computing show decreasing improvements in single-thread performance, but much more of these threads become available though. Furthermore, local non-convergence (e.g. a failing screw) can be handled without convergence problems in the structural model. It also has the potential to mutually reinforce so-called hybrid fire testing/simulation (see Sauca *et al.*, 2020, 2021; Sauca, 2022). Namely, often fire tests relate to single members (or here: screw connections), whereas larger structures with these single members, too expensive to test, behave differently. With hybrid testing, this is solved by experiments for the most critical parts, real-time combined by e.g. OpenFresco with simulations for the other (surrounding) parts (see Khan *et al.*, 2020). Alternatively, also the experiments can be simulated by dedicated models, leading to virtual hybrid approaches (e.g. see Cai *et al.*, 2022).

The two-scale method (so including the small- and global-scale models) has successfully been implemented in two-way coupled fire-structure simulations (Xu *et al.*, 2021, 2023). However, as will be shown, for the method critical remarks should be made on the failure criteria for pull-out, and also combined load cases and elevated temperatures need more research. Code and scripts are available for all simulations presented in this paper, so they can be reproduced and improved further (see bso-toolbox zenodo, 2023).

2. Two-scale method

The two-scale method as presented here consists of two models: a small-scale model and a global-scale model. The small-scale model simulates the screw connection in relative detail, such that its essential behaviour is described, and it provides the characteristics (i.e. stiffness) of the springs that model the screws in the global-scale model. The global-scale model simulates the structural system, and thermal and mechanical conditions around the screw connection are transferred to the small-scale model via so-called submodelling (introduced in Section 2.1). The small-scale and global-scale models are mutually coupled, as further explained in Section 2.2. Finally, within the small-scale model, a proprietary technique is used to model the behaviour of the threads, so they need not be modelled explicitly, as introduced in Section 2.3.

2.1 Submodelling

Data transfers from the global-scale to the small-scale models are carried out by submodelling, which was originally conceived to remodel a region of a finite element model by a refined mesh for a detailed solution in that region (see e.g. Bogdanovich and Kizhakkethara, 1999). Here, submodelling is used as available in the finite element program Abaqus (2014), but similar functionality is present in most other finite element packages. Regarding submodelling, the translational and rotational values of the Degrees Of Freedom (DOF) from the "image" boundaries, at the imaginary boundaries of the small-scale model as projected on the global-scale

model, are interpolated to the coincident "driven" boundaries of the small-scale model. Two different methods can be used for the interpolation, depending on the element types used: (a) solid to solid, in case solid elements are used both in the small- and global-scale model; (b) shell to solid, in case shell elements are used in the global-scale model while solid elements are present in the small-scale model. The accuracy of these two interpolation methods has been verified by several benchmarks (Abaqus (2014)). However, the specific implementation of submodelling as used here cannot transfer temperature DOFs, and data transfers from the small- to the global-scale model cannot be handled too. This needs additional developments, as presented next.

2.2 Interaction of small and global-scale models

As common for (non-linear) finite element analyses, the two-scale method divides a structural analysis into several load steps. Here, specifically for the two-scale method, each load step consists of five analysis steps, as shown in Figure 1, and elaborated below.

(1) Global-scale model load step: A thermomechanical analysis of the global-scale model is carried out. Each screw connection in the global-scale model is represented by a non-linear elastic spring element, with three DOFs, being the displacements along the Cartesian coordinate system axes as shown in Figure 2 on the left. To make the screw connection in the global-scale model as realistic as possible (despite the use of a simple spring), drilling holes are present, and two so-called distributed coupling zones are used. The first one is the yellow ring on the top surface of Plate 1 (see Figure 2), for which its outer diameter equals the diameter of the screw head; the second one is the orange ring along the drilling hole circumference of Plate 2. Both zones are completely rigid and also rigidly connected to the spring's upper and lower nodes respectively. The spring's initial axial stiffness k_s is predicted by Leston-Jones *et al.* (1997):

$$k_s = \frac{E_s \cdot A_s}{l_s} \tag{1}$$

in which E_s is Young's modulus for the screw at a given temperature, A_s is the stress area of the screw shank's cross-section, and l_s is the screw's elongation length. Young's modulus is generally taken as 210,000 N/mm^2, and for the elongation length the screw length is selected. For the other two (tangential) directions, the initial stiffness is assumed to be one-third of the axial stiffness. Note that these values are only meant to initiate the simulations, and will quickly be replaced, after the first load step, by actual values from the small-scale model.

(2) Transfer of boundary conditions and temperatures: Using submodelling as introduced in Section 2.1, the values of translational and rotational DOFs of the global-scale model at the imaginary "image" boundary of the small-scale model, are applied to the "driven" boundaries of the small-scale model. Because the screw connection is only a small part

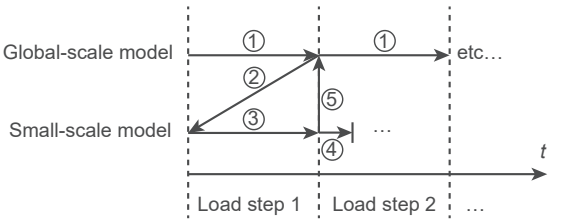

Figure 1.
Timeline for the two-scale method

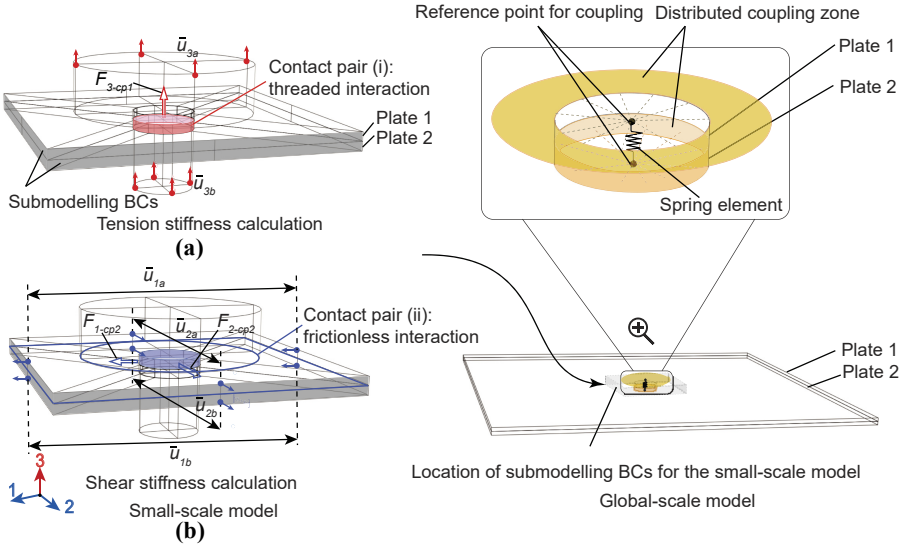

Figure 2. Calculation of equivalent spring stiffness for screw connections

of the overall structural system, the average temperature (vs time) data of the two nodes of the spring element in the global-scale model are applied to the complete geometry of the small-scale model.

(3) Small-scale model load step: During this step, a detailed thermomechanical analysis of the small-scale model is conducted, using the boundary conditions and temperatures in time from the global-scale model.

(4) Stiffness prediction: After completion of the small-scale model load step, a so-called probe step is applied: All (translational) boundary conditions are simultaneously perturbed by a 1% multiplication. Resulting reaction force increments can be used to determine the momentary stiffness as follows. In general, a tangent spring stiffness can be expressed by Hooke's law:

$$k = \frac{\Delta F}{\Delta u} \tag{2}$$

where k is the tangential spring stiffness, and ΔF and Δu are variations of the load and elongation of the spring respectively.This expression can be used for the small-scale model in Figure 2 on the left. Two contact pairs are used for measuring the reaction forces F in the small-scale model. First, contact pair (i) is used, which is the (red) contact area between the inner "lining" of the hole in Plate 2 and the screw shank, and defined by "threaded connection interaction" (see Section 2.3). This contact pair is used for measuring the tension force F_{3-cp1}. Concerning displacements in this direction, the measuring points used are shown in red. The average displacements of these points on respectively the screw head and tip are defined as $\overline{u}_{3a}$ and $\overline{u}_{3b}$. These can be used to calculate the elongation of the screw as $\overline{u}_3 = \overline{u}_{3a} - \overline{u}_{3b}$. Second, contact pair (ii) is used, which consists of two surface interactions. The first surface interaction is the (blue) contact area between the inner lining of the hole in Plate 1 and the screw shank, defined by frictionless interaction, so no screw longitudinal or rotational friction can occur. Its second surface interaction is the surface in between the screw

head and Plate 1, visualised by its blue circumference (only by a circle, not an area, to not obscure the first surface interaction), again defined by frictionless interaction. Contact pair (ii) is used for measuring the forces in the tangential 1-direction F_{1-cp2} and 2-direction F_{2-cp2} (indicated blue in the figure). Corresponding displacements are taken from the plates as shown by the blue points. Thus the shear deformation in the tangential 1-direction can be found by $\overline{u}_1 = \overline{u}_{1a} - \overline{u}_{1b}$, where $\overline{u}_{1a}$ is the average (not the distance in between) of the two displacements of the top Plate 1, and $\overline{u}_{1b}$ the average of values of the bottom Plate 2. For the tangential 2-directional equivalent definitions apply. Note that also between the plates, frictionless interaction is defined. Using the information above, for each direction, ΔF in equation (2) is found by the difference of the related contact force (e.g. F_{3-cp1} for direction 3) before and after the probe step. Similarly, Δu can be found by the difference between the related $\overline{u}$ values before and after the probe step. Note that if multiple screws are present, steps (3) and (4) involve several small-scale models that can be evaluated simultaneously, by parallel computing.

(5) The tangent spring stiffness is used for the next load step of the global-scale model: As new stiffness values have been found for the screw in step 4, the spring element in the global-scale model is updated accordingly, and the global-scale model is restarted following analysis step (1) for the next load step. Steps 1 to 5 will be repeated until all load steps have been carried out.

Note that only the spring stiffness is brought back to the global-scale model, and not the tractions along the plate edges in the small-scale model, these tractions potentially influencing the displacements of the edges in the global-scale model. By Saint-Venant's principle, this needs not to be an issue, but only if the plates in the small-scale model are large enough compared to the screw. This was studied in a sensitivity study in Xu *et al.* (2023). Finally, the load step size may influence the accuracy of the predictions, indeed as will be shown in upcoming simulations. If several small-scale models are used, the most critical small-scale model will determine the step size.

2.3 Threaded connection interaction

Screw fasteners are designed to connect (to other) parts via their threads. However, modelling a screw fastener with its threads requires an extremely fine mesh, resulting in high computational costs. As the small-scale model is envisioned to be as simple as possible, nevertheless describing essential screw connection behaviour for fire-structure simulations, instead of modelling the threads explicitly, a proprietary "threaded connection interaction" model is used (Abaqus (2014)). The idea of this interaction model is to capture thread behaviour by generating forces on the screw shank and its surround (in this case the plate hole). These forces are related by a theoretical model to the threads, specified by their pitch size, thread angle, and a vector that indicates the screw's longitudinal axis. The performance of the model will be verified and validated in the next section.

3. Verification and validation of "threaded connection interaction"

In this section, "threaded connection interaction" is verified by a finite element model that models the threads explicitly. Due to its axisymmetrical character, the model with threads does not describe the thread's helical orientation, as such not considering the relationship between longitudinal loads and a rotational frictional force between the threads. The resulting error in the longitudinal load is negligible, as shown in Measurement of pitch diameter of screw thread gages (1923) and Chen and Shih (1999). In Section 3.3, "threaded

connection interaction" is validated by comparison with pull-out experiments from the literature. All simulations in this Section 3 are under ambient temperatures.

3.1 Setup of finite element models

Figure 3 on the left shows the axisymmetric finite element model with threads, and on the right, an axisymmetric model is shown using "threaded connection interaction". Each model consists of two parts: a part of the screw and a part of a plate. Note that the models are only meant to specifically verify the zone of "threaded connection interaction". Other aspects, e.g. shear or bearing failure, are treated in the upcoming sections. Therefore, in the models here some parts are absent or schematically modelled only. Finally, to study the transition from thread to shank failure, and so to include and enforce thread failure, the outer diameter has been tuned to be 16 mm, so quite larger than a normal screw.

For the model with threads, contact between the threads is defined by general (i.e. no specification of surfaces needed) contact involving the Abaqus (2014) penalty friction model with a coefficient of 0.3 in the tangential direction, and "hard contact" in the axial and radial directions. For the model with threaded connection interaction, by definition, the interaction is only defined in the normal direction, i.e. for tension. For shear, in the tangential direction, therefore an additional "surface to surface" interaction is modelled, with the same properties as defined for the general contact above. Boundary conditions (indicated in blue) apply to the outer surface of the plate, which is completely fixed, and a prescribed upwards displacement is defined to the screw shank.

The material properties for both the screw and the adjacent plate are shown at the top right, with Young's modulus E, yield strength f_y, ultimate tensile strength f_u, and ultimate tensile strain ε_u. A ductile damage model is used (Abaqus (2014)), with settings as shown in the figure, to indicate failure. Solutions are found by an implicit static solver, with automatic time stepping. And simulations stop either when the prescribed displacement reaches the specified value, or the model fails by element deletions related to the damage model.

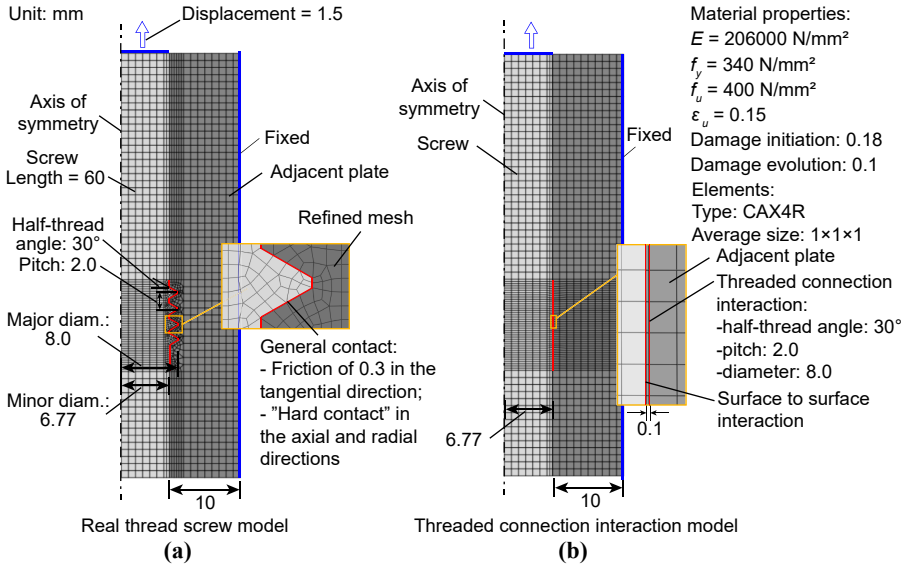

Figure 3. Axi-symmetrical finite element models with (a) threads modelled (without their helical shape) and (b) "threaded connection interaction"

3.2 Verification by real thread model

Using the above setup, screws have been simulated with one, two, three, or four threads respectively, to investigate both thread and shank tension (necking) failures. Results are shown in Figure 4, including contour plots of the plastic strains at the last increment.

Elastic stiffness is similar for both models for all cases. For one and two threads, in the real thread model failure is related to yielding of the screw thread base, and some additional yielding at the surface of the plate, just above the thread. For the threaded connection interaction model, yielding can be seen around the screw-plate boundary. Both models predict the same load-deformation behaviour qualitatively, however, for a single thread the threaded connection interaction model overestimates the strength. The simulations end due to convergence issues as soon as elements should be deleted based on the ductile damage model. For three and four threads, failure is related to the yielding of the screw shank, and both models show comparable results, both for their load-displacement behaviour, and qualitatively as shown by the contour plots. Here, simulations end when the prescribed displacement is reached.

It can be concluded that for two or more (assumed non-helical) threads in contact, threaded connection interaction is a useable substitution for modelling real threads: Elastic stiffness predictions are good, and also failure is predicted well, both qualitatively and quantitatively. For one thread, threaded connection interaction can be used for qualitative studies, however, the ultimate load is then predicted too high.

3.3 Validation by existing experiments

In the previous section, two failure modes showed up, namely thread failure and shank tension failure (necking). However, screw connections as applied in thin-walled structures

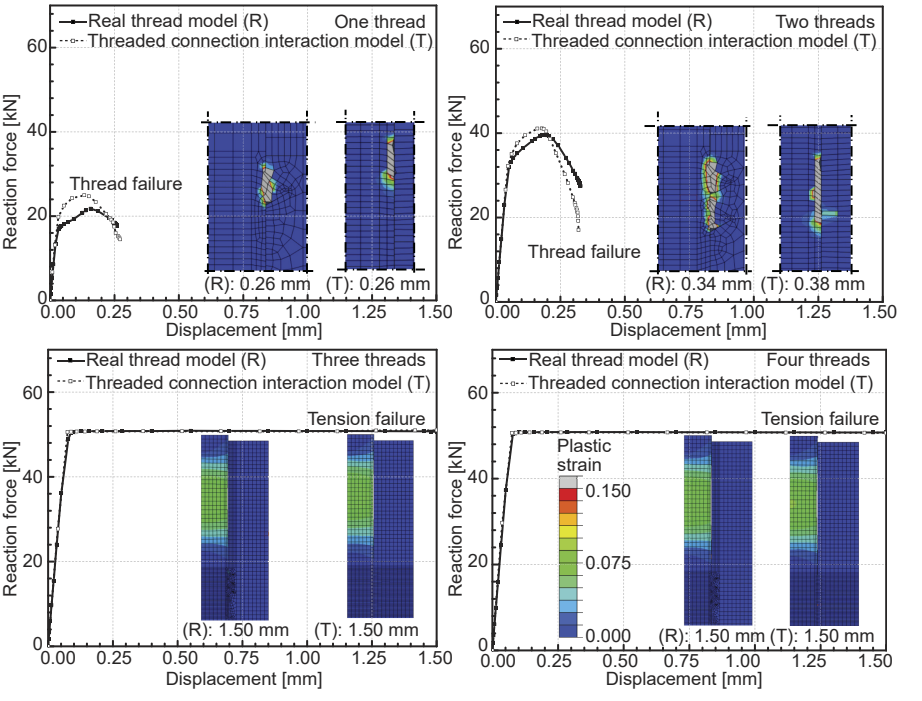

Figure 4.
Verification of threaded connection interaction with a real thread model

often have a limited number of threads in contact with the thin plates, which can lead to so-called pull-out failure. This kind of failure may even lead to the complete loss of thin-walled steel roofing systems. Related, Sivapathasundaram and Mahendran (2018) conducted 187 small-scale pull-out tests, which showed screw connections failing by pull-out, either with or without significant plate bending near the screw, depending on the ratio of plate thickness to thread pitch. To check "threaded connection interaction" also for pull-out failures, three types of their experiments are simulated here, using low-strength steel battens and 10g-16 (Teks) screws, see the first three rows in Table 4 of Sivapathasundaram and Mahendran (2018). A finite element model has been developed accordingly, using threaded connection interaction (see Figure 5).

The model consists of a screw positioned in the centre of a 100 × 100 mm plate. The screw diameter modelled is the outer thread diameter. Three types of (thin-walled) plates are used, each having a specific thickness t, yield strength f_y, and ultimate strength f_u, as shown in the figure. Measured engineering stress and strain from the experiments are converted to true stress and strain before being used in the simulation (see Section 4.1). The four edges of the plate are fully fixed, and a prescribed upwards displacement of 5 mm is uniformly applied to the screw head. Results are shown in Figure 6. Note that only ultimate loads are available in the experimental report, so horizontal lines are used for these.

Whereas the limited formulation (no threads) model predicts the trend of the experimental ultimate (pull-out) loads reasonably well, also the failure mechanism is described correctly by the finite element model: The experiments clearly show pull-out behaviour, which is

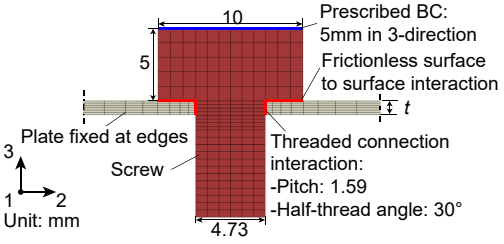

Elements:
-Type: C3D8R
-Average size: 0.5×0.5×0.5

Experiment ID Screw/plate t [mm]	Engineering f_y [N/mm²]	Engineering f_u [N/mm²]
Teks 10g-16/0.38	358	415
Teks 10g-16/0.54	359	399
Teks 10g-16/0.95	332	390

Figure 5.
Validation model for threaded connection interaction and pull-out failure

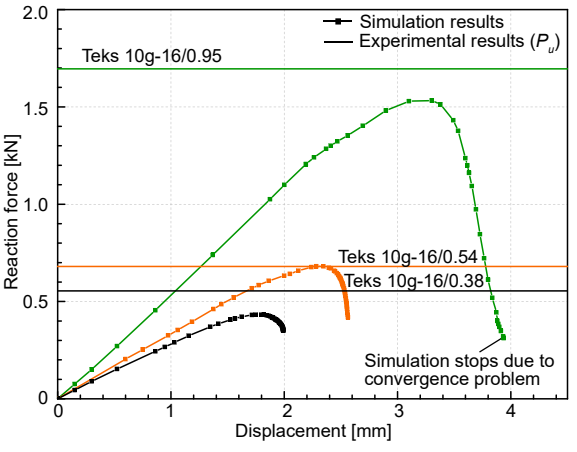

Pull-out bending failure from the experiment (4075 Batten and 12g-24 Teks) Sivapathasundaram *et al.* (2018)

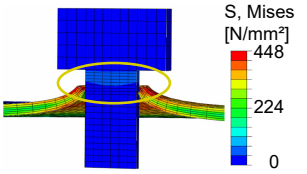

Pull-out bending deformation from simulation (t = 0.95 mm, displacement = 3.9 mm)

Figure 6.
Pull-out failure for threaded connection interaction model and experimental results from Sivapathasundaram and Mahendran (2018)

characterized by plastic bending along the circumference of the drilled plate hole, gradually widening the circular hole to such an extent that the screw threads lose their grip (see Figure 6 on the right). The same behaviour is found in the finite element model, and so "threaded connection interaction" can simulate the reduction of interlock of the threads due to the increasing diameter of the hole. This is all the more surprising as less than one full thread is in contact with the plate, as can be seen by comparing the plate thickness and the thread pitch. Note that also for these simulations material degradation is modelled, however, element deletion of the screw or plate (e.g. fracture) was not observed.

To further verify the threaded connection interaction model for pull-out failure, Eurocode EN 1993-1-3 (2006) predicts the pull-out resistance $F_{p;Rd}$ by:

$$F_{p;Rd} = 0.45tdf_u, \ (t/p < 1) \tag{3}$$

$$F_{p;Rd} = 0.65tdf_u, \ (t/p > 1) \tag{4}$$

in which f_u is the ultimate tensile strength of the plate material; d is the thread outer diameter; t is the plate thickness; and p is the thread pitch. For the experiments of Sivapathasundaram and Mahendran (2018) these equations lead to 0.336, 0.459, and 0.789 kN for the experiments with $t = 0.38$, 0.54, and 0.95 mm respectively, the numbers indicating a very conservative Eurocode: On average the experiments show a 1.75 times larger ultimate load than Eurocode. As the model and experiments agree better, and similar findings concerning the design code were reported by Mahendran and Tang (1998), further pull-out cases will not be verified by the Eurocode directly.

In summary, it has been shown that for a thick plate, for an increasing number of threads, a screw connection first fails by thread failure and then by shank tension failure (necking), Section 3.2. For a thin plate, pull-out failure may occur, as presented in this section. All these failure modes are strongly related to the screw threads, and a finite element model using "threaded connection interaction" can predict the failure modes reasonably well. As mentioned earlier, for a single thread failure, some quantitative differences exist between the models with thread and "threaded connection interaction".

4. Verification of the two-scale method

Now that critical parts of the small-scale model have been explained, verified, and validated in Section 3, the two-scale method, as introduced in Section 2, will be demonstrated for the four most typical failure modes (at ambient temperatures) as suggested by Eurocode EN 1999-1-4 (2011): bearing, shear, tension, and pull-out.

Firstly, note that the Eurocode for aluminium structures is adopted, since, differently from the steel-based EN 1993-1-3 (2006) it does not need tests for tension and shear resistance predictions, and still allows the use of steel plates, thus providing a single consistent set of formulae.

Secondly, three similarly named failure modes are pull-out, pull-through, and pull-over, here using the definitions as shown by Marković *et al.* (2012). Pull-out has been shown in Section 3.3. For pull-through, the screw remains in place, but the plate it supposes to fix loosens by a circular shear failure around the screw head, effectively bypassing the screw. A similar failure is pull-over, however, now the plate around the screw head bends plastically, as such widening the screw hole. Both European design codes EN 1999-1-4 (2011) and EN 1993-1-3 (2006) only treat pull-out and pull-through, whereas the North American Specification AISI S100-16 (2020) only lists pull-out and pull-over. Possibly, these documents combine pull-through and pull-over in a single definition, and to avoid further issues, in this paper it is assumed that large enough screw heads or washers are used to avoid pull-through and pull-over failures.

Verification of the two-scale method for the four failure modes takes place by a so-called detailed system model and the EN 1999-1-4 (2011) design rules.

4.1 Setup of finite element simulations

Two finite element models are used in this section: A detailed system model, as shown in Figure 7 on the left, and the two-scale method, as shown in the centre. The detailed system model is only meant for verification, and models two plates and a connecting screw, all in full detail, but using "threaded connection interaction" instead of threads. As mentioned earlier in Section 2, the two-scale method uses a global-scale model that models the plates in full detail (but without drilled threads) and applies a spring element for the screw. The stiffness properties of the spring element are obtained from a small-scale model, modelling the screw in more detail. For the small-scale model, a size of 30 × 30 mm is taken for the plates, based on a sensitivity study in Xu *et al.* (2023). Related, the mesh density of the small-scale model is based on existing models in the literature, see the introduction, and an (undocumented) sensitivity study, for both bolts and screws, using various validating experiments, e.g. as used in this paper.

Concerning the boundary conditions, the four edges of Plate 2 (yellow in the figure) are fixed for all DOFs, and the four (red) edges of Plate 1 have a prescribed displacement, for which the direction and value depend on the investigated failure mode, as specified in the figure on the right. Regarding contact interactions, the threaded connection interaction model is used in between the (screw-drilled) hole of plate 2 and the screw shank (see also Section 2.3). For all other surfaces potentially in contact, a general (i.e. no specific surfaces need to be addressed) contact property is defined as frictionless and with hard contact.

The ambient material properties are taken either as C3 stainless steel as suggested for connections by EN ISO 3506-1:2009 (2009), or steel S355 as defined by a yet unpublished Eurocode prEN 1993-1-14 (2023). Temperature-dependent behaviour of the materials, only used in Section 4.3, is based on EN 1993-1-2 (2005). Finally, when finite elements show a total strain of 0.15, they are assumed to fail, using the ductile damage model introduced in Section 3.1. Note that following EN 1993-1-2 (2005) this is for all temperatures, however, in reality, allowable strains will be much higher for elevated temperatures. This will be discussed further in Section 4.3. The engineering stress-strain relations (σ_{eng}, ε_{eng}) are converted into true stress-strain (σ_{true}, ε_{true}) values by:

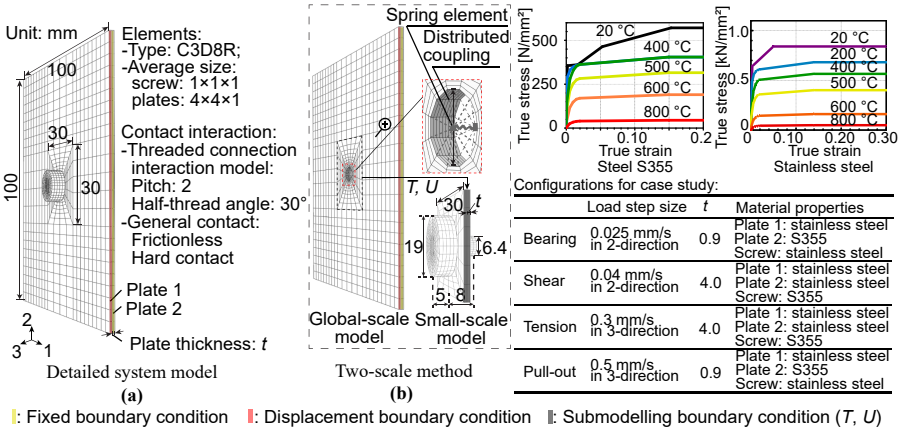

Figure 7.
Setup of the detailed system model (left), two-scale method (centre), and material properties and configurations (right)

$$\sigma_{true} = \sigma_{eng}(1 + \varepsilon_{eng}) \tag{5}$$

$$\varepsilon_{true} = \ln(1 + \varepsilon_{eng}) \tag{6}$$

And the resulting stress-strain curves are indicated in Figure 7 at the top right. To provoke different failure modes, different materials and plate thicknesses (always equal for both plates) are used, see the table of configurations in Figure 7.

4.2 Verification of the two-scale method by the detailed system model and the Eurocode

In this section, the two-scale method will be verified by the detailed system model and Eurocode predictions. Results of the simulations, as introduced in the previous section, are shown in Figure 8.

Bearing is here the plastic elongation of a screw drilled hole in a plate, and for the case investigated, Eurocode EN 1999-1-4 (2011) predicts bearing resistance at ambient temperature as:

$$F_{b;Rd} = 1.5 f_u dt = 1.5 \times 490 \times 6.4 \times 0.9 = 4.2 \text{ kN} \tag{7}$$

in which $F_{b;Rd}$ is the bearing resistance, $f_u = 490$ N/mm^2 is the (engineering) ultimate tensile strength of Plate 2, d is the screw diameter, and t is the plate thickness. Using the material

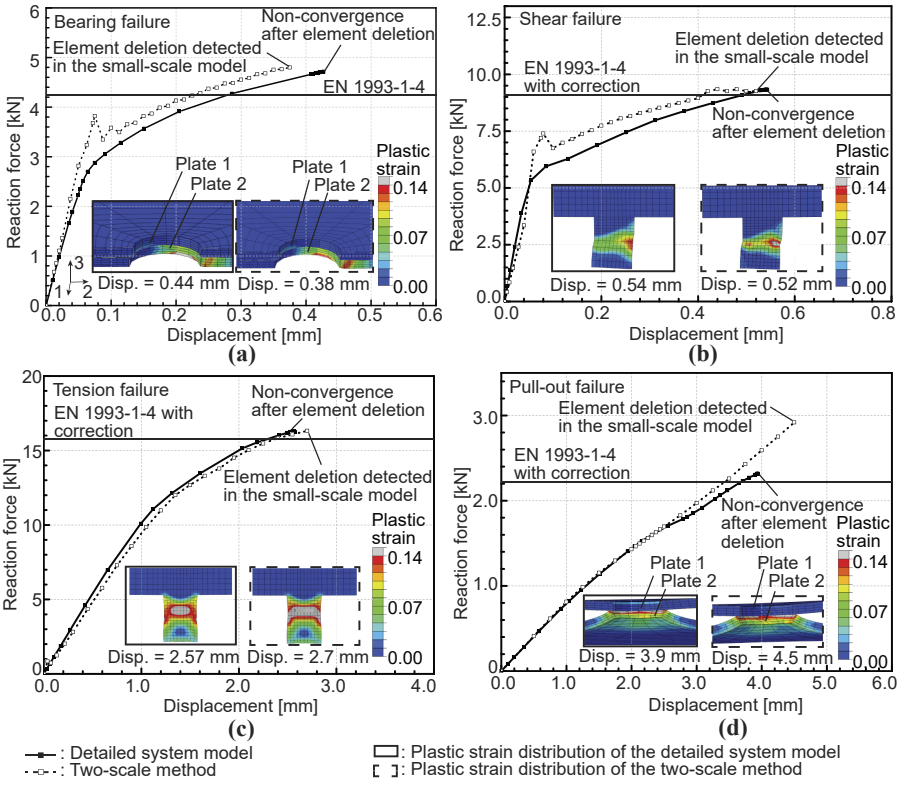

Figure 8.
Two-scale method vs detailed system model and Eurocode predictions for different failure modes

models introduced in Section 4.1, force-displacement curves are obtained as given in Figure 8(a). The two-scale method shows slightly stiffer elastic behaviour than the detailed system model. This is probably caused by the screw-drilled holes in the global-scale model being rigid along their circumference (see also Figure 2). Nevertheless, thanks to the small-scale model describing bearing behaviour, the two-scale method can capture the behaviour of the detailed system model well. Only for abrupt stiffness changes (e.g. from the elastic to the plastic stage), the two-scale method needs a subsequent load step, where the stiffness is updated, to be on track again. Using smaller load steps will resolve this issue if required. Bearing failure occurs in Plate 2 first, where strongly reduced stiffness of the failed finite elements leads to convergence problems in the detailed system model. Differently, in the two-scale method, the simulation is programmed to stop in a controlled way as soon as the small-scale model detects failed finite elements. Contour plots on the deformed geometry show a similar plastic strain distribution for both models too. Finally, the models agree reasonably well with the prediction of Eurocode EN 1999-1-4 (2011), although formally the Eurocode equation is only valid for plates with an ultimate tensile strength smaller than 250 N/mm^2.

Another mode is the shear failure of the screw. Naturally, this occurs for thicker plates, which do not easily tear by shear. Therefore, in the simulations now strong plates (here "stainless steel") with a thickness equal to 4.0 mm are used, together with a lower-strength S355 screw. Simulation results are shown in Figure 8(b). In addition, the shear resistance of a screw connection in EN 1999-1-4 (2011) is given by:

$$F_{v;Rd} = \frac{490}{\sqrt{3}} A_s = 282.9 \times \pi \times 3.2^2 = 9.1 \text{ kN} \tag{8}$$

in which $F_{v;Rd}$ is the shear resistance and A_s is the cross-sectional area of the screw shank. Note that normally this equation uses an assumed shear strength of the steel equal to 380 N/mm^2, but here the actual material values have been used. Results show slight differences in elastic stiffness for the two models, as explained for bearing. After elastic and elastoplastic behaviour, as soon as the displacement is close to 0.52 mm, some finite elements in the screw shank start to degrade, and consequently convergence problems occur for the detailed system model. In general, the two-scale method shows a similar force-displacement curve as the (verifying) detailed system model, and both models show shearing of the screw as the failure mode.

Figure 8(c) shows the results for the shank tension failure mode (necking), for which Eurocode EN 1999-1-4 (2011) gives the following design equation:

$$F_{t;Rd} = 490 A_s = 490 \times \pi \times 3.2^2 = 15.8 \text{ kN} \tag{9}$$

where $F_{t;Rd}$ is the tension resistance and A_s is the stress area (here equal to the modelled area) of the screw shank. Note that normally this equation uses an assumed tensile strength of the steel equal to 560 N/mm^2, but here the actual material values have been used. Again, the two-scale method is verified satisfactorily by the detailed system model, including failure: As soon as the screw reaches its tension capacity, due to finite elements in the screw shank that start to fail (see the grey elements in the middle of the screw shank), the detailed system model becomes unstable, and convergence problems occur. Also, plastic strain distributions are very similar for both models.

The final failure mode to present is pull-out, in which plate bending and tangential stretching result in the widening of the screw drilled hole, so the screw threads lose their grip. Section 3.3 showed that such behaviour can be simulated by the detailed system model (using threaded connection interaction), so the two-scale method can be verified with the detailed system model here too. Simulation results are shown in Figure 8(d). In the elastic stage, the two-scale method shows the same behaviour as the detailed system model. However, for

displacements larger than 2.5 mm, the two-scale method is somewhat stiffer. This is due to the global-scale model having a rigid hole circumference, which caused similar issues for bearing. For the plastic strain distribution, the final state of both models is presented, and these are similar for the two models. However, different from Section 3.3, the load-deformation behaviour does not show a peak, and also the contour plots do not show actual pull-out. Note that both cases are different: in Section 3.3 the screw is pulled and so all parts in the simulations are displacement controlled, whereas here Plate 1 is pulled and the screw is not completely constrained, so possibly exhibits rigid body motion. If equation (3) from Section 3.3 is used, Eurocode EN 1999-1-4 (2011) predicts a pull-out load equal to 1.27 kN. As shown by the models and experiments in Section 3.3 this is on average 1.75 times too low a prediction, so the system is expected to fail approximately at 2.22 kN. So here it may be the case that element deletions forecast pull-out, although in Section 3.3 material degradation and element deletions were not present at all. This needs further research.

For all four failure modes, bearing, shear, tension, and pull-out, load-deformation behaviour and failure predictions of the two-scale method are verified by the detailed system model. Eurocode EN 1999-1-4 (2011) agrees reasonably well with all failure modes too, taking into account the actual strength of the material, and a serious correction for pull-out, the latter rightfully based on finite element models and experiments. Also qualitatively, all failure modes are captured, although pull-out failure needs further research. In the next section, the two-scale method will be validated for combined load actions, among others via existing experiments, and demonstrated for different temperatures.

4.3 Validation for load combinations and demonstration of temperature loads

Concerning a validation for load combinations, Francka and LaBoube (2009) conducted an experimental study in which screw connections were subject to tension pull-out and shear forces. For each experiment, a cold-formed steel deck section (304.8 mm × 304.8 mm, with two top flanges, a bottom flange, and four webs) was fixed in the middle of the bottom flange by a screw to a cold-formed steel flat sheet, with dimensions 50.8 mm (normal-ductility steel) or 101.6 mm (low-ductility steel) × 152.4 mm. Via a test fixture, tension was applied to the deck section and flat sheet under different angles between the deck and vertical (tensile) axis (15, 30, 60, and 75°) so to deliver decreasing amounts of shear relative to tension. For low angles (15 and 30°) a few times the screw failed by shear, and these experiments were removed from the results. The remaining experiments all failed by combined pull-out and bearing of the sheet, accompanied by tilting of the screw.

To simulate experiment 16N14-15 in Francka and LaBoube (2009), the detailed system model and two-scale method as presented in Section 4.1 are used, with the following remarks. A No. 14 screw was used in the experiment, its diameter quite close to the width of the screw in the existing model, so this is unmodified, similar to the value of the half-thread angle. However, the pitch size (assumed to be 14 TPI) is set to 1.8 mm now. As only Plate 2 (see Figure 7) fails in the experiments, Plate 1 is left unmodified, whereas the thickness of Plate 2 is changed to 1.3 mm, and its material properties are taken from table 3.1 in Francka and LaBoube (2009), with yield stress = 277 N/mm^2, ultimate stress = 336 N/mm^2, and ultimate strain = 0.3. Regarding the displacement boundary conditions applied on the edges of Plate 1, for the 15-degree experiment, the load step size is 0.112 mm in the 2-direction (tension direction) and 0.03 mm in the 3-direction (shear direction).

Results of the detailed system model and the two-scale method are shown in Figure 9(a), together with dotted lines indicating the envelope of experimental results, as in general only ultimate loads were reported (which applies to other test programs used in this paper too). For a few experiments, load-deformation graphs are available but cannot be used for validation, since deformations of the test fixture, deck, and plate are unknown for the

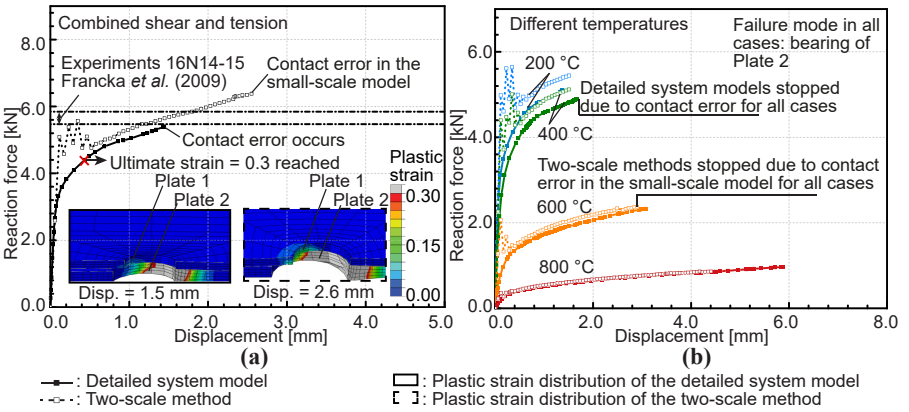

Figure 9.
(a) Experiments and (b) different temperature loads, two-scale method vs detailed system model

experiments and not modelled either (again this also applies to other validations in this paper). Note that the displacement shown along the horizontal axis is the vector sum of the two displacement components, and the same applies to the reaction force on the vertical axis.

If for these simulations, at ambient temperature, the first occurrence of a principal total tensile strain equal to 0.3 is assumed to indicate failure, the simulations are very conservative (see the red cross in the figure). This can be understood, as for bearing a first very small crack will not indicate ongoing stretching of the hole, as also shown in the figure by the contours on the deformed geometry. Therefore, the simulations in Figure 9(a) have been carried out without the ductile damage model (which would use the 0.3 strain for failure). As such, the detailed system model stops around 1.5 mm displacement due to contact errors that result in non-convergence. The two-scale method follows the detailed system model and continues further, but similarly, contact errors in the global-scale model cause non-convergence around 2.6 mm. As shown by the deformed meshes at the final step, significant bearing takes place, also the screw tilts (not shown), but no visible pull-out of the screw can be seen. Principally, contact errors and a subsequent failure to converge are not an indication of failure, nevertheless, the results suggest a correlation. To investigate this further, some more experiments are simulated, as shown in Figure 10. All simulations stop due to contact errors

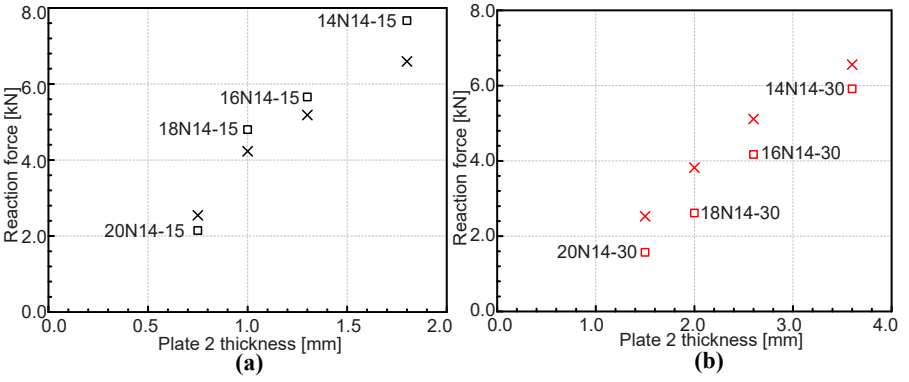

Figure 10.
Experiments and simulations for (a) 15-degree (more shear) and (b) 30-degree angles (less shear)

followed by non-convergence, which for all cases correlates quite well with experimental failure. An explanation may relate to the fact that in the simulation the screw is a rigid body, only fixed by the contact definitions. As such, a possible initiation of pull-out leads to singularities and so non-convergence.

Recall that in Section 3.3, a small-scale model with threaded connection interaction was able to describe pull-out decently, with no convergence issues. Differently, in Section 4.2 actual pull-out was not observed, but element deletion caused by final stage material degradation correlated with (corrected) Eurocode predictions. Finally, in this Section 4.3, a quite convincing correlation can be found between contact errors and experimental failure. However, experimental failure means here a combination of pull-out and bearing, and in the finite element models only bearing was observed. All in all, simulations of pull-out failure are far from consistent and need further research.

As a demonstration, the above simulations are also carried out under temperatures of a constant 200 °C, 400 °C, 600 °C, and 800 °C for all parts. Temperature-dependent material properties are used as presented in Section 4.1. However, also here no ductile damage model is used, since (a) allowable strains vary significantly for elevated temperatures and (b) the ultimate tensile strain was not a good marker of failure for the ambient simulations (Figure 9(a)). Furthermore, thermal expansion was not taken into account, because for future use in two-way coupled fire-structure analyses, it is believed that thermal expansion effects are needed on the global scale, but likely need not be modelled on the small-scale, to be researched. Results are shown in Figure 9(b), and as a general conclusion the two-scale method and detailed system model show similar load-displacement curves. Likewise as for the ambient case, for all temperatures, bearing, and no pull-out, is observed, and both the detailed system model and two-scale method stop due to contact errors and subsequent convergence issues. Assuming this as an indication of failure, see above, higher temperatures lower the strength, but in return provide more ductility, as expected.

4.4 Two-scale method in two-way coupled fire-structure simulations

The two-scale method has been shown to predict all essential failure modes quantitatively and qualitatively, although the latter inconsistently for pull-out. It also has been verified for a combined load case, and tested for temperature loads. This allows a demonstration of the two-scale method to include essential screw connection behaviour in two-way coupled fire-structure simulations. This demonstration was first presented in Xu *et al.* (2021), and an overview is given in Figure 11.

The demonstration comprises a building compartment, with its façade being a single sandwich panel, fixed to two C-section steel columns via four screws. The simulation is divided into load steps (see Section 2.2). During each load step, first a Fire Dynamics Simulation (FDS) is carried out and the resulting Adiabatic Surface Temperature (AST) data is transferred to the FEM domain for a heat transfer analysis. This analysis provides the temperature distribution (in time) of the sandwich panel and the C-columns. Hereafter, a thermomechanical (structural response) analysis is carried out. In terms of the two-scale method, this all relates to the global-scale model: the sandwich panel and C-section columns, connected by spring elements. Note that the global-scale model also includes thermal expansion following Eurocode EN 1993-1-2 (2005). Then, submodelling and temperature boundary conditions are transferred to four small-scale models, one for each screw. Structural responses of the small-scale models are obtained, i.e. stiffness and failure. For demonstration purposes, the complete sandwich panel is assumed to fail if two (out of four) screw connections fail. Once this is the case, the panel is removed for subsequent fire simulation load steps. Naturally, this changes the fire scenario significantly, as shown in the figure. As such, a two-way coupled simulation has been carried out. In the future, more detailed simulations

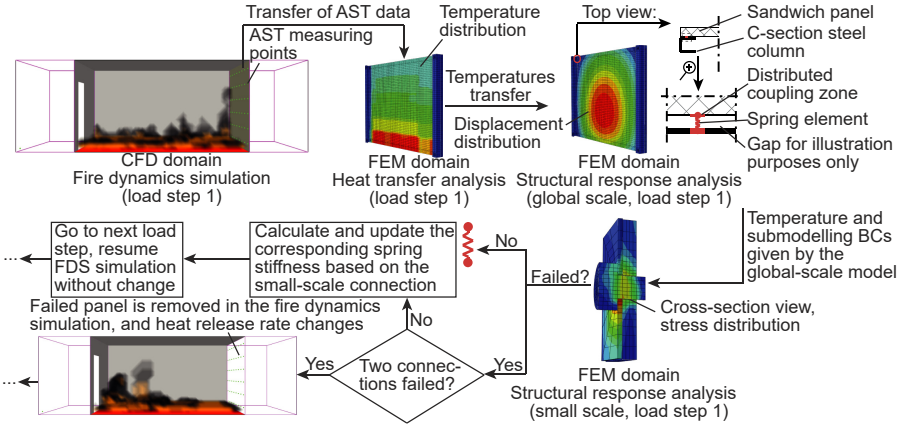

Figure 11.
Two-scale method in a coupled fire-structure simulation

(e.g. more panels and connections, and including pyrolysis) can be tried, following Feenstra *et al.* (2018) and De Boer *et al.* (2019).

5. Conclusions

To predict the essential behaviour (stiffness and failure) of screw connections in structures, when subject to various load conditions and temperatures, a two-scale method has been proposed. It consists of (a) a global-scale model that relates to the overall structural system and (b) a small-scale model to describe a screw connection. Components in the global-scale model are connected by a spring element instead of a modelled screw, and the stiffness of this spring element is predicted by the small-scale model, updated at each load step.

To avoid the computationally expensive modelling of the threads, the small-scale model uses a proprietary technique "threaded connection interaction" to model the behaviour of the thread, which was (a) verified by a model that models the complete thread geometry, and (b) validated by pull-out experiments. It was shown that "threaded connection interaction" can predict all the for this thread study relevant failure modes, i.e. thread failure, shank tension failure (necking), and pull-out.

The applicability of the two-scale method has been shown by the verification of all relevant types of screw connection failure, namely bearing, shear, tension, and pull-out failure. For all four failure modes, load-deformation behaviour and failure predictions of the two-scale method were verified by a detailed system model. Eurocode EN 1999-1-4 (2011) agrees reasonably well with the failure modes too, taking into account a serious correction for pull-out, justified by finite element models and experiments.

Additionally, the two-scale method was validated for a combined load case by existing experiments, and demonstrated for different temperatures. For a variety of experiments, a good correlation has been found between experimental and simulation results. And by assuming contact problems in the simulations as an indication of failure, it has been shown that higher temperatures lower the strength, but in return provide more ductility, as expected.

Pull-out simulations were shown to be inconsistent, which needs further research: In one case a small-scale model with threaded connection interaction was able to describe pull-out, whereas for another case only element deletion caused by final stage material degradation correlated with (corrected) Eurocode predictions. And if damage modelling was switched off, a quite convincing correlation was found between contact errors and experimental bearing/

pull-out failure. It could be investigated whether suppressing rigid-body displacements of the screw would help.

A case of a building compartment with a sandwich panel system under fire was mentioned. It demonstrated the implementation of the two-scale method in a two-way coupled fire-structure simulation.

For two-way coupled fire-structure simulations, the two-scale method is a significant improvement over the spring elements used currently: The method is insightful, for it contains a functional separation of scales, revealing their relationships (e.g. screws are fully modelled, yet their representative stiffness can be monitored explicitly), and it is computationally efficient as it allows for distributed computing. Furthermore, local small-scale non-convergence (e.g. a screw failing) can be handled without convergence problems in the global-scale structural model. The method may also be useful for densely packed screw configurations: if many screws in a regular pattern fix the same plates, it may be tried to let a single small-scale model be representative for all of them, clearly limiting the computational costs, and this approach could be studied for different parameters. If screws behave differently or see different boundary conditions, then each screw needs a small-scale model. This will not save absolute computational costs, but small-scale models can be distributed across different threads or CPUs, which dramatically reduces wall clock time.

Although a promising method, more research is needed before the two-scale method can be used under all circumstances. Further investigations should pursue better-defined failure criteria for pull-out, and the study of more and different combined load cases, under temperature loads. Code and scripts are available for all simulations presented in this paper, so can be reproduced and improved further (see bso-toolbox zenodo, 2023).

References

Abaqus (2014), *Abaqus Analysis User's Guide*, Version 6.14, Dassault Systèmes Simulia Corp., Providence, RI.

AISI S100-16 (2020), *North American Specification for the Design of Cold-Formed Steel Structural Members*, American Iron and Steel Institute, Washington, DC.

Al-Jabri, K.S. (2004), "Component-based model of the behaviour of flexible end-plate connections at elevated temperatures", *Composite Structures*, Vol. 66 No. 1, pp. 215-221.

Bogdanovich, A. and Kizhakkethara, I. (1999), "Three-dimensional finite element analysis of double-lap composite adhesive bonded joint using submodeling approach", *Composites Part B: Engineering*, Vol. 30 No. 6, pp. 537-551.

bso-toolbox zenodo (2023), "TUe-excellent-buildings/journal_paper_fire_testing _two_scale_simulations_panels_connections: code_and_scripts", Zenodo, v.1.0.1, doi: 10.5281/zenodo.7977268.

Cábová, K., Garifullin, M., Mofrad, A.S., Wald, F., Mela, K. and Ciupack, Y. (2021), "Shear resistance of sandwich panel connection at elevated temperature", *Journal of Structural Fire Engineering*, Vol. 13 No. 2, pp. 162-170.

Cai, X., Jiang, L., Qiu, J., Orabi, M.A., Yang, C., Lou, G., Khan, M., Yuan, Y., Li, G. and Usmani, A. (2022), "Dual-3d hybrid fire simulation for modelling steel structures in fire with column failure", *Journal of Constructional Steel Research*, Vol. 197, 107511.

Chen, J.-J. and Shih, Y.-S. (1999), "A study of the helical effect on the thread connection by three dimensional finite element analysis", *Nuclear Engineering and Design*, Vol. 191 No. 2, pp. 109-116.

De Boer, J.G.G.M., Hofmeyer, H., Maljaars, J. and van Herpen, R.A.P. (2019), "Two-way coupled CFD fire and thermomechanical FE analyses of a self-supporting sandwich panel façade system", *Fire Safety Journal*, Vol. 105, pp. 154-168.

EN 1993-1-2 (2005), *Eurocode 3: Design of Steel Structures - Part 1-2: General Rules: Structural Fire Design*, European Committee for Standardization, Brussels.

EN 1993-1-3 (2006), *Eurocode 3: Design of Steel Structures - Part 1-3: General Rules-Supplementary Rules for Cold-Formed Members and Sheeting*, European Committee for Standardization, Brussels.

EN 1999-1-4 (2011), *Eurocode 9: Design of Aluminium Structures - Part 1-4: Cold-Formed Structural Sheeting*, European Committee for Standardization, Brussels.

EN ISO 3506-1:2009 (2009), *Mechanical Properties of Corrosion-Resistant Stainless Steel Fasteners — Part 1: Bolts, Screws and Studs*, European Committee for Standardization, Brussels.

EN ISO 898-1-2013 (2013), *Mechanical Properties of Fasteners Made of Carbon Steel and Alloy Steel — Part 1: Bolts, Screws and Studs with Specified Property Classes — Coarse Thread and Fine Pitch Thread*, European Committee for Standardization, Brussels.

Feenstra, J.A., Hofmeyer, H., Van Herpen, R.A.P. and Mahendran, M. (2018), "Automated two-way coupling of CFD fire simulations to thermomechanical FE analyses at the overall structural level", *Fire Safety Journal*, Vol. 96, pp. 165-175.

Fischer, E.C., Chicchi, R. and Choe, L. (2021), "Review of research on the fire behavior of simple shear connections", *Fire Technology*, Vol. 57 No. 4, pp. 1519-1540.

Francka, R.M. and LaBoube, R.A. (2009), *Screw Connections Subject to Tension Pull-Out and Shear Force, Research Report RP09-3*, American Iron and Steel Institute, Washington, DC.

Huynh, M.T., Pham, C.H. and Hancock, G.J. (2020), "Experimental behaviour and modelling of screwed connections of high strength sheet steels in shear", *Thin-Walled Structures*, Vol. 146, 106357.

Jiang, J., Jiang, L., Kotsovinos, P., Zhang, J., Usmani, A., McKenna, F. and Li, G.-Q. (2015), "Opensees software architecture for the analysis of structures in fire", *Journal of Computing in Civil Engineering*, Vol. 29, 04014030.

Khan, M.A., Jiang, L., Cashell, K.A. and Usmani, A. (2020), "Virtual hybrid simulation of beams with web openings in fire", *Journal of Structural Fire Engineering*, Vol. 11, pp. 118-134.

Kyvelou, P., Gardner, L. and Nethercot, D.A. (2017), "Design of composite cold-formed steel flooring systems", *Structures*, Vol. 12, pp. 242-252.

LaBoube, R.A. and Sokol, M.A. (2002), "Behavior of screw connections in residential construction", *Journal of Structural Engineering*, Vol. 128 No. 1, pp. 115-118.

Leston-Jones, L.C., Burgess, I.W., Lennon, T. and Plank, R.J. (1997), "Elevated-temperature moment-rotation tests on steelwork connections", *Proceedings of the Institution of Civil Engineers-Structures and Buildings*, Vol. 122 No. 4, pp. 410-419.

Lu, W., Ma, Z., Mäkeläinen, P. and Outinen, J. (2012), "Behaviour of shear connectors in cold-formed steel sheeting at ambient and elevated temperatures", *Thin-Walled Structures*, Vol. 61, pp. 229-238.

Lu, W., Mäkeläinen, P., Outinen, J. and Ma, Z. (2011), "Design of screwed steel sheeting connection at ambient and elevated temperatures", *Thin-Walled Structures*, Vol. 49 No. 12, pp. 1526-1533.

Mahendran, M. and Tang, R.B. (1998), "Pull-out strength of steel roof and wall cladding systems", *Journal of Structural Engineering*, Vol. 124 No. 10, pp. 1192-1201.

Marković, Z., Budevac, D., Dobrić, J. and Fric, N. (2012), "Specific behaviour of thin-walled member joints with fasteners", *Gradevinar*, Vol. 64, pp. 217-230.

Measurement of pitch diameter of screw thread gages (1923), Department of Commerce, Bureau of Standards, Washington, DC.

prEN 1993-1-14 (2023), *Eurocode 3 - Design of Steel Structures - Part 1-14: Design Assisted by Finite Element Analysis, in Preparation*, European Committee for Standardization, Brussels.

Roy, K., Lau, H.H., Huon Ting, T.C., Masood, R., Kumar, A. and Lim, J.B. (2019), "Experiments and finite element modelling of screw pattern of self-drilling screw connections for high strength cold-formed steel", *Thin-Walled Structures*, Vol. 145, 106393.

Sauca, A. (2022), *Hybrid Fire Testing: Past, Present and Future*, Springer International Publishing, Cham, pp. 275-304.

Sauca, A., Zhang, C., Chernovsky, A. and Seif, M. (2020), "Communication framework for hybrid fire testing: developments and applications in virtual and real environments", *Fire Safety Journal*, Vol. 111, 102937.

Sauca, A., Mortensen, N., Drustrup, A. and Abbiati, G. (2021), "Experimental validation of a hybrid fire testing framework based on dynamic relaxation", *Fire Safety Journal*, Vol. 121, 103315.

Sivapathasundaram, M. and Mahendran, M. (2016a), "Development of suitable test methods for the screw connections in cold-formed steel roof battens", *Journal of Structural Engineering*, Vol. 142 No. 6, 04016025.

Sivapathasundaram, M. and Mahendran, M. (2016b), "Experimental studies of thin-walled steel roof battens subject to pull-through failures", *Engineering Structures*, Vol. 113, pp. 388-406.

Sivapathasundaram, M. and Mahendran, M. (2018), "New pull-out capacity equations for the design of screw fastener connections in steel cladding systems", *Thin-Walled Structures*, Vol. 122, pp. 439-451.

Stamatopoulos, H. and Malo, K.A. (2020), "On strength and stiffness of screwed-in threaded rods embedded in softwood", *Construction and Building Materials*, Vol. 261, 119999.

Swanson, J.A. and Leon, R.T. (2001), "Stiffness modeling of bolted T-stub connection components", *Journal of Structural Engineering*, Vol. 127 No. 5, pp. 498-505.

Usmani, A., Zhang, J., Jiang, J., Jiang, Y. and May, I. (2012), "Using opensees for structures in fire", *Journal of Structural Fire Engineering*, Vol. 3, pp. 57-70.

Xu, Q., Hofmeyer, H. and Maljaars, J. (2021), "A two-scale FE model to address connections in coupled fire-structure simulations", in *'ASFE'21, Applications of Structural Fire Engineering 2021'*, University of Ljubljana, pp. 388-393.

Xu, Q., Hofmeyer, H. and Maljaars, J. (2023), "A two-scale model to include essential bolted connection behaviour in two-way coupled fire-structure simulations, to be submitted".

Xu, Q., Hofmeyer, H., Maljaars, J. and Van Herpen, R.A.P. (2023), "Full-Scale Fire Resistance Testing and Two-Scale Simulations of Sandwich Panels with Connections", *Fire Technology*, (In press) doi: 10.1007/s10694-023-01463-y.

Yan, S. and Young, B. (2012a), "Screwed connections of thin sheet steels at elevated temperatures – Part I: steady state tests", *Engineering Structures*, Vol. 35, pp. 234-243.

Yan, S. and Young, B. (2012b), "Screwed connections of thin sheet steels at elevated temperatures – Part II: transient state tests", *Engineering Structures*, Vol. 35, pp. 228-233.

Zoetemeijer, P. (1974), "A design method for the tension side of statically loaded, bolted beam-to-column connections", *Heron*, Vol. 20 No. 1, pp. 3-57.

Corresponding author
Hèrm Hofmeyer can be contacted at: h.hofmeyer@tue.nl